Wide-Band Inline-Amplified WDM Transmission Using PPLN-Based Optical Parametric Amplifier

Takayuki Kobayashi ⓘ, *Member, IEEE*, Shimpei Shimizu ⓘ, *Member, IEEE*, Masanori Nakamura ⓘ,
Takeshi Umeki, *Member, IEEE*, Takushi Kazama ⓘ, Ryoichi Kasahara ⓘ, Fukutaro Hamaoka ⓘ,
Munehiko Nagatani ⓘ, *Member, IEEE*, Hiroshi Yamazaki ⓘ, *Member, IEEE*, Hideyuki Nosaka ⓘ, *Member, IEEE*,
and Yutaka Miyamoto, *Member, IEEE*

(Post-Deadline Paper)

Abstract—This article proposes an optical parametric amplifier (OPA), as an inline-repeater, using a periodically-poled-LiNbO₃ (PPLN) waveguide with over-10-THz amplification bandwidth, and also presents wide-band wavelength-division-multiplexing (WDM) inline-amplified transmission with the OPA. Our PPLN-based OPA is polarization-independent and has a spectrally efficient configuration by filtering phase-conjugated signals (idlers). We implemented our PPLN-based OPA with half its ideal configuration with an over-10-THz amplification bandwidth because of the limited number of PPLN waveguides. The implemented OPA had 5.125-THz amplification bandwidth, gain of beyond 15 dB, and noise figure of less than 5.1-dB. The gain excludes the 5.6-dB loss of an idler rejection filter employed in the transmission experiment so that the implemented OPA can compensate 9.5-dB link loss of transmission fibers and optical components. A 3 × 30.8-km inline-amplified transmission with 41-channel 800-Gbps WDM signal in 125-GHz spacing was successfully demonstrated using our PPLN-based OPA as an inline-repeater. The results also indicate that the OPA's amplification bandwidth can potentially be extended to 10.25 THz.

Index Terms—800G transmission, digital coherent transmission, high-symbol-rate signal, optical communication systems, optical parametric amplifier (OPA), wavelength division multiplexing (WDM).

I. INTRODUCTION

TO INCREASE the capacity of optical communication systems, extending the available optical bandwidth and

advancing digital coherent technologies are indispensable. Extending the optical amplification bandwidth by upgrading optical repeaters, which typically consist of standard erbium-doped fiber amplifiers (EDFAs) with a 4-THz bandwidth, is attractive to increase the capacity at the deployed-fiber link. Transmission experiments involving the use of an optical bandwidth of over 10-THz have been conducted based on hybrid Raman/EDFAs [1], [2], all-Raman amplification [3], and additional optical-band utilization such as S-, C- and L-bands [4]–[6]. A semiconductor optical amplifier with over-100-nm continuous bandwidth was developed and demonstrated as a discrete optical amplifier [7]. And WDM transmission with 150-nm bandwidth using S-, C- and L-bands has been demonstrated employing discrete-Raman amplifiers [8]. New optical bands besides the S, C and L bands have also attracted attention. A bismuth-doped fiber amplifier with an amplification bandwidth of 115 nm in the O and E bands has recently been reported [9].

Optical parametric amplification via nonlinear phenomena is promising and has been studied using highly nonlinear fibers (HNLFs) or periodically poled LiNbO₃ (PPLN) waveguides [10], [11]. Amplification in an HNLF-based optical parametric amplifier (OPA) is caused by four-wave mixing (FWM) via the third-order nonlinearity of optical fibers, whereas amplification in a PPLN-based OPA is based on quasi-phase-matched (QPM) difference-frequency generation (DFG) due to the second-order nonlinearity of PPLN waveguides. They are based on different phenomena but provide the same functionality. The attractive features of an OPA are small gain-transient response [12], [13], wide band [14], [15] and high gain [16], [17], and it has applications such as spectral inversion and phase-sensitive amplification using phase-conjugated signals, namely idlers, in the process of parametric amplification. The simplest function of an OPA, phase-insensitive amplification (PIA), is promising as a discrete optical repeater with a wide amplification bandwidth.

Some studies have demonstrated inline-amplified transmission with an HNLF-based OPA. With a single-channel signal, 4×80-km dispersion-managed transmission using a single-polarization 40-Gbps on-off keying modulated signal with the OPA compensating for the span-loss compensation of 20 dB has been reported [18]. With a WDM signal, inline-amplified transmission over 25.2-km single-mode-fiber (SMF) spans using a

20-ch 50-GHz-spaced WDM signal with 100-Gbps polarization-division-multiplexed (PDM)-quadrature phase shift keying (QPSK) signals has been reported [19]; its amplification bandwidth is 1 THz. The bandwidth and gain of OPAs depend on the pump-light power and phase-matching conditions. The pump light is typically placed at the same wavelength band as the signals in HNLF-based OPAs. The high-power pump light can generate unnecessary idlers by FWM with undesirable combinations of the signals and the pump light. Thus, it is challenging to simultaneously achieve both high gain and wide bandwidth.

A PPLN-based OPA is expected to achieve low-crosstalk and wide-band amplification for a WDM signal because it is based on second-order nonlinearity, and we can use a configuration in which the high-power pump-light is not located at the signal wavelength band [20]. Wide-band performances for an optical phase conjugation have been reported: 2.5-THz WDM signal using 10-Gbps OOK format [15] and 2-THz WDM signal using PDM-16QAM format [21]. PPLN waveguides have typically a broadband amplification bandwidth and its further extension can be achieved by pump detuning from QPM wavelength [22]. However, conversion efficiency and pump power has been limited by photorefractive effect depending on fabrication methods for PPLN waveguides. For overcoming those limitations, it is a promising solution to employ directly-bonded PPLN ridge waveguide fabricated using dry etching technology [23]. The conversion efficiency of PPLN waveguides has been continuously improved; therefore, high gain over 30 dB has been achieved [17]. We have recently demonstrated inline-amplified WDM transmission using a PPLN-based OPA, which can amplify an over-5-THz WDM signal, as an inline optical repeater [24].

This paper describes our proposed PPLN-based OPA and the inline-amplified WDM transmission using the OPA, as an extended version of our previous work [24]. High-conversion-efficient PPLN modules provide an over-10-THz amplification bandwidth, gain of beyond 15 dB, and noise figure (NF) of less than 5.1-dB. We implemented the PPLN-based OPA with half proposed ideal configuration and demonstrated for the first time inline-amplified 5.125-THz WDM transmission with a PPLN-based phase-insensitive OPA by using 41-ch 800-Gb/s polarization-division-multiplexed (PDM) probabilistically shaped (PS)-36QAM signals within a 125-GHz-spaced WDM slot. A re-circulating transmission repeating three 30.8-km spans also confirmed that a PPLN-based OPA as an inline-amplifier can potentially extend the amplification bandwidth to over 10 THz.

II. PPLN-BASED OPTICAL PARAMETRIC AMPLIFIER

A. Spectral-Efficient OPA

In phase-insensitive amplification, an undesirable idler is generated in principle, and the spectral efficiency of transmission systems is halved. Therefore, a spectrally efficient configuration is required. Fig. 1 shows the conceptual configuration of our spectrally efficient OPA. It is very similar to the optical phase conjugator [25], but the difference is whether the signal or idler is suppressed. This configuration using
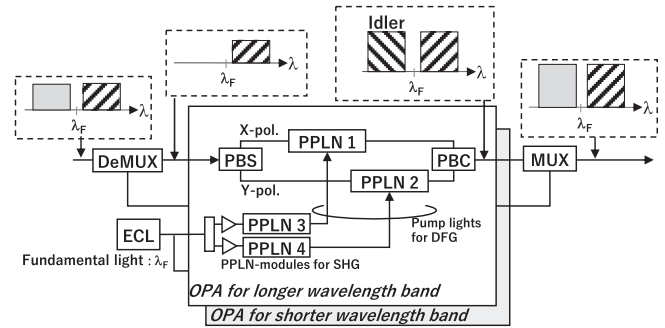

Fig. 1.   Conceptual configuration of proposed PPLN-based OPA.

in-house high-conversion-efficient and wide-band PPLN waveguides [23] offers polarization-independent amplification with an over-10-THz bandwidth. In our OPA, longer wavelength (slash-pattern) and shorter wavelength (solid) bands are separately amplified after band-dividing with the demultiplexing (De-MUX) filter. The 2-stage configuration [20] is used to construct the OPA because it can provide amplification without the undesired optical parametric process. The term "2 stage" means that the pump-light generation for the DFG and signal amplification through the DFG are processed independently by using dedicated PPLN modules. In the amplification of a longer wavelength band, two PPLN modules (PPLN 1 & 2) are used to achieve optical parametric amplification of the polarization tributaries of X and Y via the DFG. The other PPLN modules (PPLN 3 & 4) are used to generate pump lights for signal amplification. This pump-light generation is based on second harmonic generation (SHG). The pumping light for SHG is located at the center of the amplification bandwidth of a PPLN-waveguide. It is called "fundamental light", and its wavelength is denoted as λ_F. The input WDM signal is divided into two polarization tributaries by using a polarization beam splitter (PBS) and fed into a PPLN module at each polarization lane. After parametric amplification, the amplified signals and the idler (backslash-pattern) of both polarization components are combined using a polarization beam combiner (PBC). The amplification process in the short wavelength band is the same as that in the long wavelength band except that the amplification band is different. Finally, the MUX filter combines the two amplified bands while rejecting the unnecessary idlers. The amplification bandwidth is not continuous and usually divided into 2 bands. This configuration requires a guard-band around the fundamental light wavelength because a signal crossing the fundamental wavelength is not properly amplified and the MUX and DeMUX filters require a transition band. The conceptual configuration requires a pump laser, eight PPLN modules, two pairs of PBS/PBC, MUX/DeMUX filters, pump combiners, and four high-power EDFAs to achieve over-10-THz bandwidth and polarization-independent amplification. They are discretely connected. The temperature control of the PPLN modules is also required for stable operation. This is currently more complicated compared with mature amplifiers such as Raman amplifier and EDFA. To be comparable with them, further advances are required such as an integration of optical components, sharing of PPLN modules for SHG as well as improvement of conversion efficiency of PPLN-waveguide.
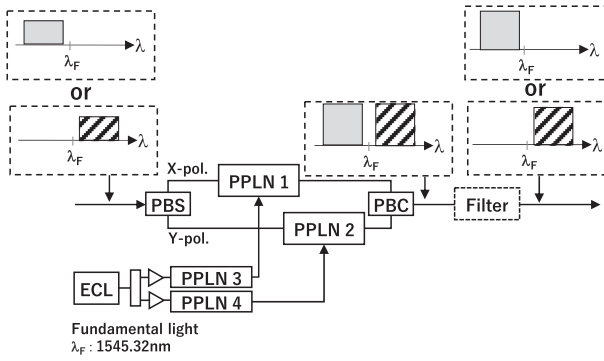
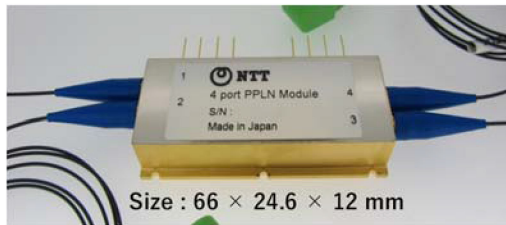Fig. 2.   PPLN-based OPA implemented for transmission experiment.

Fig. 3.   4-port PPLN-module for OPA (PPLN 1, 2).

Fig. 2 shows the implementation of our PPLN-based OPA for the transmission experiment described in the following section. A total of eight PPLN-modules are required to implement the ideal OPA configuration shown in Fig. 1; however, we implemented only half this configuration, which can amplify either longer- or shorter- wavelength bands because the number of PPLN-modules were limited to four. An in-house 4-port PPLN-module for signal amplification is shown in Fig. 3. It is very compact $66 \times 24.6 \times 12$ mm, and one PPLN waveguide is packaged with optical assemblies such as a pump/signal combiner. An external-cavity laser (ECL) with 5-kHz linewidth is used as the fundamental light source for SHG; its wavelength is 1545.32 nm (194 THz). The MUX and DeMUX filters are not included because they were implemented as a part of the re-circulating loop for the transmission experiment. The following measurements were conducted with the OPA's configuration shown in Fig. 2.

B. CW Light Amplification Characteristics

The gain and NF of our OPA are shown in Fig. 4 and exclude the losses of the MUX/DeMUX filters. They are measured at the output of the PBC by sweeping the wavelength of continuous-wave (CW) light with the input power of -25 dBm. The pumping power to each PPLN-module for SHG was set to $\sim$2 W, and 125-GHz guard-band was inserted at each side of the fundamental light wavelength of 1545.32 nm. For a bandwidth extension, QPM wavelength was detuned by temperature control. At the wavelength range of 1504 to 1588 nm, 10.2-THz amplification bandwidth, over-15-dB gain, and flat NF spectra around 5 dB were achieved. Note that actual OPA's gain, i.e., the capability of loss compensation of transmission link, strongly depend on the losses of MUX/DeMUX filters, and higher loss of DeMUX
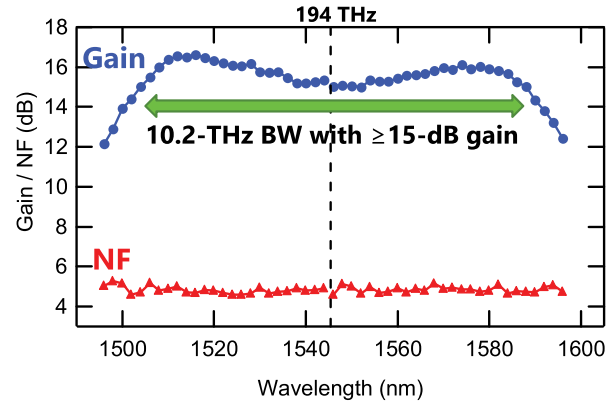
Fig. 4.   Gain and NF spectra of the PPLN-based OPA without MUX/DeMUX filters.
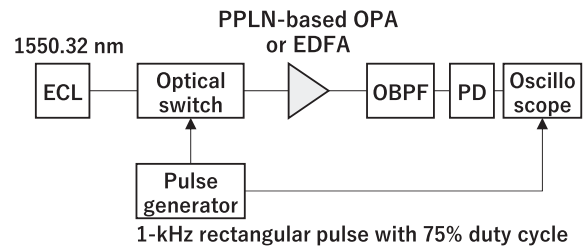
Fig. 5.   Measurement setup for transient effect of our PPLN-based OPA and conventional EDFA.
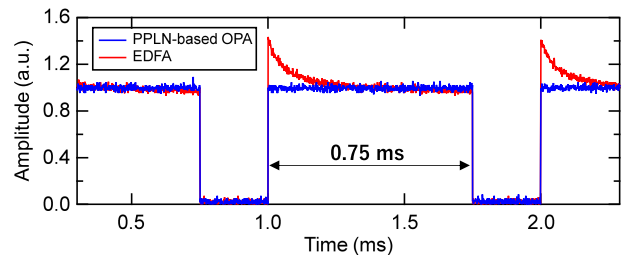
Fig. 6.   Transient effect of our PPLN-based OPA and EDFA.

filters degrades the NF. Lower losses of them would be required for an implementation of an inline-amplifier.

Next, the transient effect of our OPA was investigated and compared with that of a conventional EDFA. This is very important for gain variation due to the add/drop/switch of wavelength paths at the optical node. The measurement setup is shown in Fig. 5. CW light with a wavelength of 1550.32 nm from the ECL was pulsed with an optical switch driven by a rectangular pulse with a frequency of 1 kHz and duty cycle of 75% and was input to either the OPA or EDFA at an input power of -10 dBm. The gains of both amplifiers were set to 15 dB. The amplified signal was extracted with an optical bandpass filter (OBPF) with 1-nm bandwidth. After optical-to-electrical conversion with a photo detector (PD), the waveforms of the amplified signals were observed with an oscilloscope. Fig. 6 shows the measurement results of the transient responses of the OPA and EDFA. The amplitude response of the OPA was rectangular without any overshoot of its amplitude because of the femtosecond-scale response of the parametric process in the

Fig. 7.　Experimental setup.

Fig. 8.　Schematic of spectrum transition in re-circulating loop: (A) input of loop, (B) output of OPA, and (C) output of wavelength blocker.

PPLN waveguide. OPA via a PPLN waveguide is caused by an interaction between lights and electron in the nonlinear medium. It is based on the mechanism of dielectric polarization which has a fast response time of $\sim 10^{-15}$ sec [26]. On the other hand, expected overshoot of amplitude was observed in the EDFA, and it took several-hundred μs for amplitude convergence due to its slow response time of ~ 1 ms via stimulated emission. The results indicate that our OPA can be applied as an in-line amplifier placed at optical nodes in flexible optical networks as well as increase the available optical bandwidth.

III. TRANSMISSION EXPERIMENTS

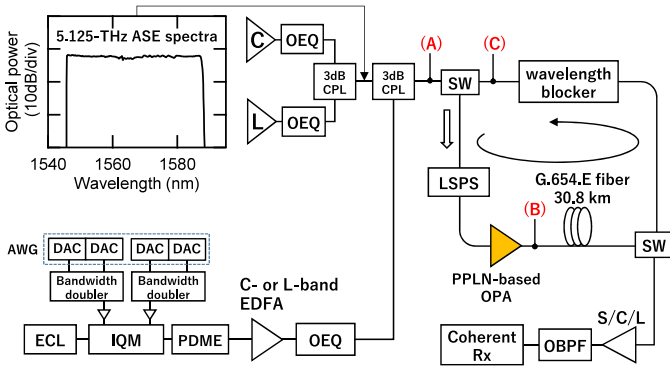This section details the inline-amplified transmission experiment with our PPLN-based OPA as an optical repeater. 800-Gbps PDM-PS-36QAM signals with 125-GHz WDM spacing were used as validating signals.

A. Experimental Setup

Fig. 7 shows the experimental setup. For validating inline-amplified transmission, a WDM signal of a 5.125-THz optical bandwidth corresponding to a 125-GHz-spaced 41-ch signal consisted of a measurement signal and amplified spontaneous emission (ASE)-based interference signal. A Nyquist-pulse-shaped 120-Gbaud PS-36QAM signal for measurement was generated using an IQ-modulator (IQM) driven by bandwidth-doubler-based high-speed digital-to-analog converters (DACs) [27], [28]. An arbitrary waveform generator with four DACs were used as sub-DACs for the bandwidth doublers. Sub-DACs had a 3-dB bandwidth of 32 GHz and were operated at 96 GS/s with pre-processed waveform data. The offline digital pre-processing included error correction of transmitter components in addition to signal spectra processing for the bandwidth doubler. The output signal of each bandwidth doubler was equivalently operated at a 192-GS/s sampling rate with doubled bandwidth of the sub-DACs. The 64QAM was truncated to 36QAM for reducing its peak-to-average power ratio, and the symbol distribution was probabilistically shaped to a Maxwell-Boltzmann distribution for achieving the target information rate of 4.435. We used the concatenated code of low-density parity check and Bose-Chaudhuri-Hocquenghem (BCH) codes with a code rate of 0.826. Assuming 1.64% pilot-signal insertion, a net data rate of the signal after PDM by using a PDM emulator (PDME) was 800
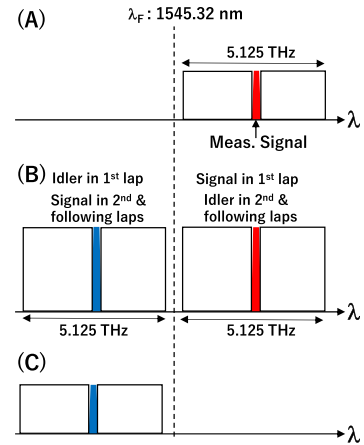
Gb/s. It was calculated from [2 pol. × {4.4375 bit/symbol – (1 – 0.826) × 6 bit/symbol} / 1.0164 × 120 Gbaud]. Further details of the signal design are described in a previous study [29]. After amplification with either a C- or L-band EDFA according to its wavelength, the measurement signal was optically equalized to enhance the high-frequency component [30] and eliminate ASE simultaneously. To emulate a 41-channel 125-GHz-spaced WDM signal, ASE was loaded to the 5.125-THz optical band from 1505.55 to 1587.25 nm except the wavelength of the measurement signal [31]. Flat and broadband ASE spectra, which are shown in the inset of Fig. 7, were achieved by coupling using a 3-dB coupler after spectral shaping of the EDFA output with an optical gain equalizer (OEQ) at each C- and L-band. The ASE with 125-GHz bandwidth at the measurement WDM channel was rectangularly suppressed with the OEQs. The measurement signal was coupled with the interfering WDM signal using a 3-dB coupler while adjusting spectral power densities of the two signals. The WDM signal was then fed into the re-circulating loop. The measurements regarding wavelength dependence was conducted by sweeping the wavelength of the modulated signal and notched position of ASE.

The transmission line consisted of a re-circulating loop containing a 30.8-km G.654.E fiber with a 125-μm^2 effective area, loop-synchronous polarization scrambler (LSPS), optical switches (SWs), a wavelength blocker, and our PPLN-based OPA. The OPA with 15-dB gain compensated for the losses of the transmission fiber (5.6 dB at 1550 nm), wavelength blocker (5.5 dB), and other loop components. The transmission fiber length in the loop was mainly restricted by the insertion loss of the wavelength blocker which played a role of MUX/DeMUX filters explained in section II. Ideally, they should be implemented in the OPA. Fig. 8 shows a schematic of the transition of the WDM signal spectra at each point, (A), (B) and (C), in the loop shown in Fig. 7. In the first lap, the OPA played the role of a post-amplifier and amplified the 5.125-THz WDM signal. Consequently, a 10.25-THz WDM signal was achieved and contained the amplified WDM signal at a longer wavelength than that of the fundamental light of λ_F (1545.32 nm) and its idler at shorter wavelength than λ_F shown in Fig. 8(B). After 30.8-km fiber transmission, the wavelength blocker suppressed

the longer-wavelength signals, and the 41 shorter wavelength signals were re-circulated. In the second and following laps, the wavelength blocker suppressed the longer-wavelength signals, and the 41 shorter-wavelength signals were input to the OPA playing the role of an inline-amplifier. The reason to suppress the longer-wavelength signals was because the wavelength blocker's pass-band was limited to the wavelength range of S and C bands. Because of the limitation in the number of PPLN modules, the amplification bandwidth was restricted to half the ideal configuration of the OPA. In the loop, no optical gain equalizer was used.

At the receiver side, the measurement signal dropped from the loop by an optical switch was amplified with an S-, C- or L-band rare-earth-doped fiber amplifier according to the wavelength of the signal. EDFAs were used for the C- and L-bands, and a thulium-doped fiber amplifier (TDFA) was used for the S-band. Next, the measurement signal was extracted using a tunable OBPF. It was then detected by a polarization-diversity intradyne coherent receiver containing a PLC-based dual polarization optical hybrid, four balanced PDs, and a digital storage oscilloscope. A free-running ECL with a linewidth of ~70 kHz was used as a local oscillator. The received signal was digitized using ADCs at 200 GS/s with 70-GHz bandwidth and post-processed off-line with a complex 8×2 MIMO equalizer [32]. The signal was demodulated using a pilot-aided adaptation algorithm [33]. After frontend error correction with a fixed linear equalizer, the chromatic dispersion was compensated by frequency domain equalization. Polarization de-multiplexing and signal equalization were realized by T/2-spaced complex 8×2 MIMO adaptive FIR filters enabling the compensation of the transmitter imperfection in receiver-side DSP under the existence of frequency offset between lasers in transmitter and receiver. The carrier frequency offset was compensated by a digital PLL. Adaptive DSP functions were pre-converged in data-aided mode using least-mean square (LMS) criteria. Then, a decision-directed LMS algorithm and pilot-aided LMS algorithm were employed for tracking in the data symbols where pilot symbols were periodically inserted. Bit wise log-likelihood ratios (LLRs) were calculated by bit-metric decoding applied to each recovered symbol. Finally, the normalized generalized mutual information (NGMI) for the PS-36QAM was computed with the LLRs. We used the NGMI threshold of 0.857 of the outer BCH code [32] as criteria of signal quality.

B. Results

We first measured the input power causing gain saturation in a back-to-back configuration. Either a 5.125-THz WDM or single-channel signal was input to the OPA. The total input power was varied from −9 to 7 dBm in 2-dB increments. The wavelength of the validating signal was 1553.33 nm in both cases. In the WDM case, it corresponded to varying the averaged channel power from to −25 to −9 dBm/λ. As shown in Fig. 9, gradual gain saturation was observed in both signals. However, nonlinear distortion on the signals was not observed at the measured input-power region, as show in the constellation diagrams in the inset of Fig. 9.Note that, nonlinear distortions can be occurred at higher input-power region in our OPA.
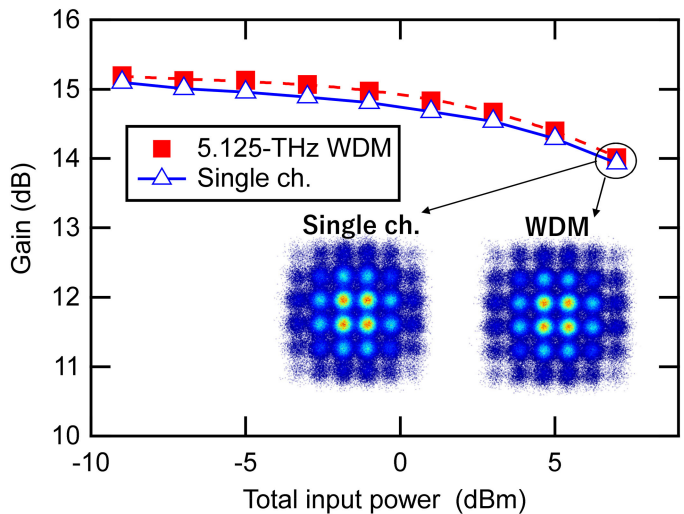

Fig. 9. Gain saturation in single channel and WDM signals.
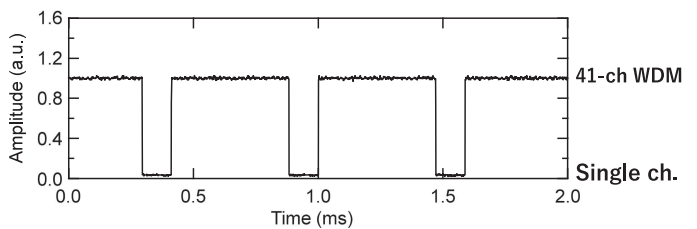

Fig. 10. Gain-transient effect in switching input signal to OPA between single channel and 41-ch WDM configurations.

We then investigated the gain-transient effect when the number of WDM channels was changed. Fig. 10 shows the gain-transient effect in switching the number of WDM channel inputs to the OPA between 1 and 41 by turning on and off the ASE-based interfering signal with an optical shutter placed before the 3-dB coupler. This corresponds to the change in the amplification bandwidth from 125 GHz to 5.125 THz. No gain-overshoot was observed as in CW light measurement described in Section II. This result indicates that this fast response can relax the requirements to designing gain fluctuations due to wavelength addition/deletion and sudden link fails, although further investigation is required on whether the gain response impacts on signal quality.

Next, we investigated the dynamic range of the OPA. Regarding the dependency of amplified-signal quality on the bandwidth of an input WDM signal after 3×30.8-km transmission, as shown in Fig. 11, the input-signal bandwidth was varied by adding an interfering WDM signal of 1.875-THz in the C-band, 2.625-THz in the L-band, and 5.125-THz full loading to the measurement signal at a wavelength of 1537.4 nm. This corresponds to changing the number of WDM channels to 1, 16, 22, and 41. The signal power was set to -21 dBm per channel, and the total input power to the OPA was up to -5 dBm. In all measurements, pumping power was not changed. No significant degradation in the NGMI was observed under any condition. This indicates that the dynamic range of the OPA has at least 16 dB.

Finally, we conducted an all-channel measurement at $3 \times$ 30.8 km. We tuned the total input power to −5 dBm to the OPA
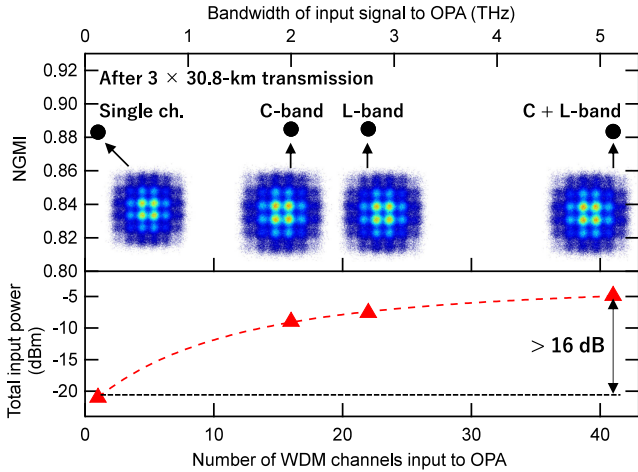
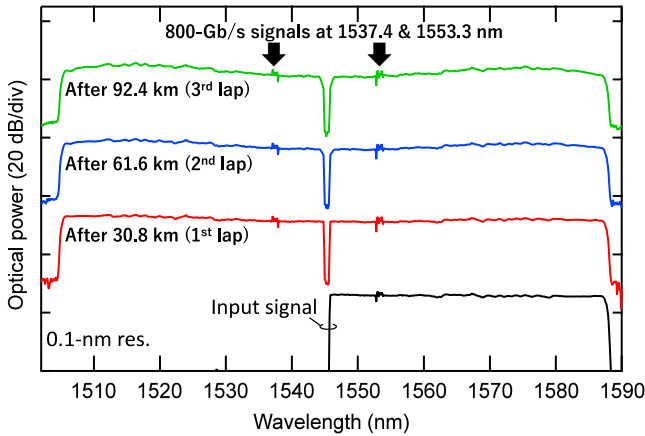Fig. 11. Dependency of amplified-signal quality on input-signal bandwidth After 3 × 30.8-km transmission.

Fig. 12. Optical spectra at output of 30.8-km fiber at 1st, 2nd, and 3rd laps.

Fig. 13. Measured NGMI of WDM channels after 92.4-km (3 × 30.8 km) transmission.
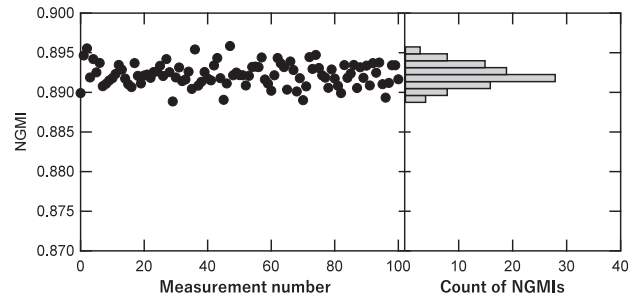
Fig. 14. Temporal dependence of NGMI (left) and its variance (right).

for achieving 15-dB gain as shown in the Fig. 9. It corresponds to an averaged channel power of −21 dBm in the 41-channel WDM configuration. Therefore, averaged fiber input power was −6 dBm/ch in the linear transmission region of 120-Gbaud WDM signal [33]. Fig. 12 shows the optical spectra at the input of the loop and the output of the fiber at each lap. In these spectra, the measurement signal was inserted to 1553.3 nm. By increasing the number of laps, the outside of the spectra was slightly raised due to the non-flat gain profile shown in Fig. 4. The maximum number of laps was set to three because there was no OEQ in the loop to maintain the flatness of the WDM signal. As explained in the previous section, the 41 channels on the wavelength band shorter than that of the fundamental light were re-circulated in the loop, and the others were newly generated idlers via the DFG at each lap. The NGMI of all channels after 92.4-km transmission is shown in Fig. 13. The NGMI of all 41 channels in each optical band was better than the NGMI threshold of 0.857, represented with a dashed line. The NGMI dependence on wavelength including the difference between the two bands is caused by the gain and NF characteristics of the optical amplifiers in the transmitter and receiver. The NGMI plunged around 1522 and 1572 nm due to the border between the amplification bandwidth of the C-band EDFA, S-band TDFA,
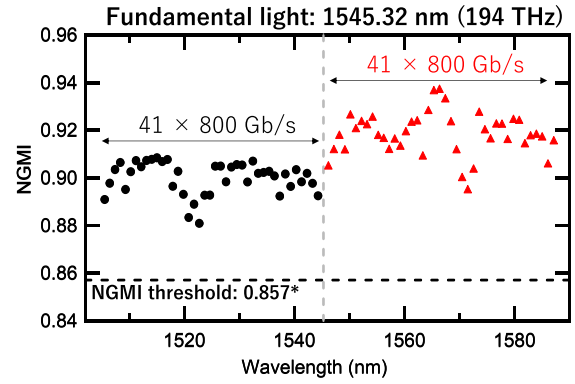
and L-band EDFA. And, the higher performance in the longer wavelength band was observed compared with that in the shorter wavelength band because of wavelength dependencies of optical components such as OBPFs, couplers, optical 90 degree hybrid and photo-detectors in the coherent receiver with the use of different optical pre-amplifiers. We also measured the stability of both polarization amplifications. Fig. 14 shows the temporal dependence and histogram of 100 measurements of the channel at the wavelength of 1537.4 nm after 92.4-km transmission. The polarization state of the input to the OPA at each measurement was changed by polarization scrambling with the LSPS. The duration between measurements was about 2 seconds. This confirms that NGMI fluctuations are sufficiently small, although the result includes all fluctuations due to the transmission system and that the worst channel never falls below the NGMI threshold.

These results indicate that 5.125-THz inline-amplified transmission with our PPLN-based OPA can be achieved, and amplification bandwidth can be potentially extended to 10.25 THz by measuring the signal quality of both signals and idlers.

IV. CONCLUSION

We proposed a PPLN-based OPA and demonstrated inline-amplified WDM transmission using 125-GHz-spaced 800-Gb/s PS-36QAM signals over 92.4-km fiber with the OPA as an inline-repeater. The PPLN-based polarization-independent OPA with half its configuration was implemented and provided a 5.125-THz amplification bandwidth with more than 15-dB gain and less than 5.1-dB NF. The measured gain and NF does not include the insertion losses of MUX/DemuX filters which

restricted the span length to 30.8 km. The extension of span length is expected by introducing the low-loss filters as well as improvement of conversion efficiency of PPLN waveguides. Fast gain-transition and 16-dB dynamic range were also confirmed. We also showed that our PPLN-based OPA can potentially extend the amplification bandwidth to over 10 THz. These results indicate that our PPLN-based OPA is promising as an in-line amplifier in future optical transport networks offering flexible utilization of wavelength resources.

REFERENCES

[1] H. Masuda *et al.*, "20.4-Tb/s (204 × 111 Gb/s) transmission over 240 km using bandwidth-maximized hybrid Raman/EDFAs," in *Proc. Opt. Fiber Commun. Conf. (OFC)*, Mar. 2007, Paper PDP20.

[2] M. Ionescu *et al.*, "74.38 Tb/s transmission over 6300 km single mode fiber with hybrid EDFA/Raman amplifiers," in *Proc. Opt. Fiber Commun. Conf. (OFC)*, Mar. 2019, Paper Tu3F.3.

[3] T. Kobayashi, A. Sano, A. Matsuura, Y. Miyamoto, and K. Ishihara, "Nonlinear tolerant spectrally-efficient transmission using PDM 64-QAM single carrier FDM with digital pilot-tone," *IEEE J. Lightw. Technol.*, vol. 30, no. 24, pp. 3805–3815, Dec. 2012.

[4] K. Fukuchi *et al.*, "10.92-Tb/s (273 × 40-Gb/s) triple-band/ultra-dense WDM optical-repeatered transmission experiment," in *Proc. Opt. Fiber Commun. Conf. (OFC)*, Mar. 2001, Paper PD24.

[5] F. Hamaoka *et al.*, "Ultra-wideband WDM transmission in S-, C-, and L-Bands using signal power optimization scheme," *IEEE J. Lightw. Technol.*, vol. 37, no. 8, pp. 1764–1771, Apr. 2019.

[6] T. Kato *et al.*, "Real-time transmission of 240×200-Gb/s signal in S+C+L triple-band WDM without S- or L-band transceivers," in *Proc. Eur. Conf. Opt. Commun. (ECOC)*, Sep. 2019, Paper PD.1.7.

[7] J. Renaudier *et al.*, "First 100-nm continuous-band WDM transmission system with 115Tb/s transport over 100km using novel ultra-wideband semiconductor optical amplifiers," in *Proc. Eur. Conf. Opt. Commun. (ECOC)*, Sep. 2017, Paper Th.PDP.A.2.

[8] M. A. Iqbal, L. Krzczanowicz, I. Phillips, P. Harper, and W. Forysiak, "150nm SCL-Band transmission through 70km SMF using Ultra-wideband Dual-stage discrete Raman amplifier," in *Proc. Opt. Fiber Commun. Conf. (OFC)*, Mar. 2020, Paper W3E.4.

[9] Y. Wang, N. Thipparapu, D. Richardson, and J. Sahu, "Broadband bismuth-doped fiber amplifier with a record 115-nm bandwidth in the O and E bands," in *Proc. Opt. Fiber Commun. Conf. (OFC)*, Mar. 2020, Paper Th4B.1.

[10] M. E. Marhic, N. Kagi, T.-K. Chiang, and L. G. Kazovsky, "Broadband fiber optical parametric amplifiers," *Opt. Lett.*, vol. 21, no. 8, pp. 573–575, 1996.

[11] K. Gallo, G. Assanto, and G. I. Stegeman, "Efficient wavelength shifting over the erbium amplifier bandwidth via cascaded second order processes in lithium niobate waveguides," *Appl. Phys. Lett.*, vol. 71, no. 8, pp. 1020–1022, Jun. 1997.

[12] G.-W. Lu, M. E. Marhic, and T. Miyazaki, "Burst-mode amplification of dynamic optical packets using fibre optical parametric amplifier in optical packet networks," *Electron. Lett.*, vol. 46, no. 11, pp. 778–780, 2010.

[13] C. B. Gaur, F. Ferreira, V. Gordeinko, A. Iqbal, W. Forysiak, and N. Doran, "Comparison of erbium, Raman and parametric optical fiber amplifiers for burst traffic in extended PON," in *Proc. Opt. Fiber Commun. Conf. (OFC)*, Mar. 2020, Paper W4B.3.

[14] T. Torounidis and P. A. Andrekson, "Broadband single-pumped fiber-optic parametric amplifiers," *IEEE Photon. Technol. Lett.*, vol. 19, no. 9, pp. 650–652, May 2007.

[15] J. Yamawaku *et al.*, "Low-crosstalk 103 channel × 10 Gb/s (1.03 Tb/s) wavelength conversion with a quasi-phase-matched linbo3 waveguide," *IEEE J. Sel. Top. Quantum Electron.*, vol. 12, no. 4, pp. 521–528, Aug. 2006.

[16] T. Torounidis, P. A. Andrekson, and B.-E. Olsson, "Fiber-optical parametric amplifier with 70-dB gain," *IEEE Photon. Technol. Lett.*, vol. 18, no. 10, pp. 1194–1196, May 2006.

[17] T. Kashiwazaki, K. Enbutsu, T. Kazama, O. Tadanaga, T. Umeki, and R. Kasahara, "Over-30-dB phase-sensitive amplification using a fiber-pigtailed PPLN waveguide module," in *Proc. Nonlinear Opt. (NLO)*, Jul. 2019, Paper NW3A.2.

[18] Z. Lali-Dastjerdi *et al.*, "Demonstration of cascaded in-line single-pump fiber optical parametric amplifiers in recirculating loop transmission," in *Proc. Eur. Conf. Opt. Commun. (ECOC)*, Sep. 2012, Paper Mo.2.C.5.

[19] M. F. C. Stephens, M. Tan, V. Gordienko, P. Harper, and N. J. Doran, "In-line and cascaded DWDM transmission using a 15 dB net-gain polarization-insensitive fiber optical parametric amplifier," *Opt. Express*, vol. 25, no. 20, pp. 24312–24325, Oct. 2017.

[20] T. Kazama, T. Umeki, M. Abe, K. Enbutsu, Y. Miyamoto, and H. Takenouchi, "Low-noise phase-sensitive amplifier for guard-band-less 16-channel DWDM signal using PPLN waveguides," in *Proc. Opt. Fiber Commun. Conf. (OFC)*, Mar. 2016, Paper M3D.1.

[21] T. Umeki *et al.*, "Simultaneous nonlinearity mitigation in 92 × 180-Gbit/s PDM-16QAM transmission over 3840 km using PPLN-based guard-band-less optical phase conjugation," *Opt. Express*, vol. 24, no. 15, pp. 16945–16951, Jul. 2016.

[22] M. H. Chou, I. Brener, K. R. Parameswaran, and M. M. Fejer, "Stability and bandwidth enhancement of difference frequency generation (DFG)-based wavelength conversion by pump detuning," *Electron. Lett.*, vol. 35, no. 12, pp. 978–980, Jun. 1999.

[23] T. Umeki, O. Tadanaga, and M. Asobe, "Highly efficient wavelength converter using direct-bonded PPZnLN ridge waveguide," *IEEE J. Quantum Electron.*, vol. 46, no. 8, pp. 1206–1213, Aug. 2010.

[24] T. Kobayashi *et al.*, "Wideband Inline-amplified WDM transmission using PPLN-based OPA with over-10-thz bandwidth," in *Proc. Opt. Fiber Commun. Conf. (OFC)*, Mar. 2020, Paper Th4C.7.

[25] T. Umeki, T. Kazama, H. Ono, Y. Miyamoto, and H. Takenouchi, "Spectrally efficient optical phase conjugation based on complementary spectral inversion for nonlinearity mitigation," in *Proc. Eur. Conf. Opt. Commun. (ECOC)*, Sep. 2015, Paper We2.6.2.

[26] G. S. He, "Nonlinear polarization of an optical medium," in *Nonlinear Optics and Photonics*. New York, NY, USA: Oxford Univ. Press, 2014, pp. 18–32.

[27] F. Hamaoka *et al.*, "120-GBaud 32QAM signal generation using ultra-broadband electrical bandwidth doubler," in *Proc. Opt. Fiber Commun. Conf. (OFC)*, Mar. 2019, Paper M2H.6.

[28] M. Nagatani *et al.*, "A beyond-1-Tb/s coherent optical transmitter front-end based on 110-GHz-bandwidth 2:1 analog multiplexer in 250-nm InP DHBT," *IEEE J. Solid-State Circuits*, vol. 55, no. 9, pp. 2301–2315, Sep. 2020.

[29] M. Nakamura *et al.*, "Entropy and symbol-rate optimized 120 GBaud PS-36QAM signal transmission over 2400 km at net-rate of 800 Gbps/λ," in *Proc. Opt. Fiber Commun. Conf. (OFC)*, 2020, Paper M4K.3.

[30] A. Matsushita, M. Nakamura, K. Horikoshi, S. Okamoto, F. Hamaoka, and Y. Kisaka, "64-GBd PDM-256QAM and 92-GBd PDM-64QAM signal generation using precise-digital-calibration aided by optical-equalization," in *Proc. Opt. Fiber Commun. Conf. (OFC)*, Mar. 2019, Paper W4B.2.

[31] D. J. Elson *et al.*, "Investigation of bandwidth loading in optical fibre transmission using amplified spontaneous emission noise," *Opt. Express*, vol. 25, no. 16, pp. 19529–19537, Aug. 2017.

[32] T. Kobayashi *et al.*, "35-Tb/s C-band transmission over 800 km employing 1-Tb/s PS-64QAM signals enhanced by complex 8 × 2 MIMO equalizer," in *Proc. Opt. Fiber Commun. Conf. (OFC)*, Mar. 2019, Paper Th4B.2.

[33] M. Nakamura *et al.*, "1.04 Tbps/carrier probabilistically shaped PDM-64QAM WDM transmission over 240 km based on electrical spectrum synthesis," in *Proc. Opt. Fiber Commun. Conf. (OFC)*, Mar. 2019, Paper M4I.4.

Takayuki Kobayashi (Member, IEEE) received the B.E., M.E., and Dr.Eng. degrees from Waseda University, Tokyo, Japan, in 2004, 2006, and 2019, respectively. In 2006, he joined NTT Network Innovation Laboratories, Yokosuka, Japan, where he was engaged in the research on high-speed and high-capacity digital coherent transmission systems. In 2014, he moved to NTT Access Network Service Systems Laboratories, Yokosuka. He had been engaged in 5G mobile optical network systems since 2016. He is currently a Distinguished Researcher with NTT Network Innovation Laboratories, where he is involved in the R&D of high-capacity optical transmission systems. His current research interests include long-haul optical transmission systems employing spectral-efficient modulation formats enhanced by digital and optical signal processing. Dr. Kobayashi is a member of the Institute of Electronics, Information and Communication Engineers (IEICE) of Japan. He has served as a Technical Program Committee (TPC) Member of the Electrical Subsystems' Category for the Optical Fiber Communication Conference (OFC) from 2016 to 2018. He has been serving as a TPC Member of the "Point-to-Point Optical Transmission" Category for the European Conference on Optical Communication (ECOC) since 2018.

Shimpei Shimizu (Member, IEEE) received the B.E. degree in engineering and the M.E. degree in information science and technology (electronics for informatics) from Hokkaido University, Sapporo, Japan, in 2016 and 2018, respectively. In 2018, he joined NTT Network Innovation Laboratories, Yokosuka, Japan. His current research interests include high-capacity optical transmission systems. He is a member of the Institute of Electronics, Information and Communication Engineers (IEICE) of Japan and the IEEE Photonics Society. He was the recipient of the 2017 IEICE Communications Society Optical Communication Systems Young Researchers Award.

Masanori Nakamura received the B.S. and M.S. degrees in applied physics from Waseda University, Tokyo, Japan, in 2011 and 2013, respectively. In 2013, he joined NTT Network Innovation Laboratories, Yokosuka, Japan. He has been engaged in the research on high-capacity optical transport networks. His research interests include digital signal processing and modulation format optimization for high-speed optical transmission. He is a member of the Institute of Electronics, Information and Communication Engineers (IEICE) of Japan. He was a recipient of the 2016 IEICE Communications Society Optical Communication Systems Young Researchers Award.

Takeshi Umeki (Member, IEEE) received the B.S. degree in physics from Gakusyuin University, Tokyo, Japan, in 2002, and the M.S. degree in physics and the Ph.D. degree in the area of nonlinear optics from the University of Tokyo, Tokyo, Japan, in 2004 and 2014, respectively. He joined NTT Photonics Laboratories, Atsugi-shi, Japan, in 2004, since then he has been involved in research on nonlinear optical devices based on periodically poled $LiNbO_3$ waveguides. Dr. Umeki is a member of the Japan Society of Applied Physics (JSAP), the Institute of Electronics, Information, and Communication Engineers (IEICE), and the IEEE/Photonics Society.

Takushi Kazama received the B.S. and M.S. degrees in electrical engineering from the University of Tokyo, Tokyo, Japan, in 2009 and 2011, respectively. In 2011, he joined NTT Device Technology Laboratories, Kanagawa, Japan, where he has been engaged in research on nonlinear optical devices based on periodically poled $LiNbO_3$ waveguides. He is a member of the Institute of Electronics, Information, and Communication Engineers of Japan (IEICE) and the Japan Society of Applied Physics (JSAP).

Ryoichi Kasahara received the B.S. degree from The University of Electro-Communications, Tokyo, Japan, in 1995 and the M.S. degree from Tohoku University, Sendai, Japan, in 1997. In 1997, he joined NTT Opto-electronics Laboratories, Ibaraki, Japan, where he was involved in research on silica-based planar lightwave circuits (PLCs), including thermo-optic switches and arrayed-waveguide grating multiplexers, and integrated optoelectrical receiver modules. He is currently with the NTT Device Technology Laboratories, Kanagawa, Japan, where he has been involved in the research and development of the fabrication technologies of optical dielectric waveguide devices. He is a Senior Member of the Institute of Electronics, Information, and Communication Engineers of Japan (IEICE) and a member of the Japan Society of Applied Physics (JSAP).

Fukutaro Hamaoka received the B.E., M.E., and Ph.D. degrees in electrical engineering from Keio University, Yokohama, Japan, in 2005, 2006, and 2009, respectively. From 2009 to 2014, he was with NTT Network Service Systems Laboratories, Musashino, Japan, where he was engaged in the research and development of high-speed optical communication systems, including digital coherent optical transmission system. He is currently with NTT Network Innovation Laboratories, Yokosuka, Japan. His research interests include high-capacity optical transport systems with ultrawideband wavelength division multiplexing and high-symbol rate techniques. Dr. Hamaoka is a member of the Institute of Electronics, Information and Communication Engineers (IEICE) of Japan. He was a recipient of the 2007 The Japan Society of Applied Physics Young Scientist Presentation Award.

Munehiko Nagatani (Member, IEEE) received the M.S. degree in electrical and electronics engineering from Sophia University, Tokyo, Japan, in 2007. In 2007, he joined NTT Photonics Laboratories, Atsugi, Japan, where he was engaged in the research and development (R&D) of ultrahigh-speed analog and mixed-signal ICs for optical communication systems. He is currently a Distinguished Researcher with NTT Device Technology Laboratories, Atsugi, Japan, and the NTT Network Innovation Laboratories, Yokosuka, Japan, where he is involved in the R&D of ultrahigh-speed ICs and systems for optical transmission using advanced modulation formats. He is a member of the Institute of Electronics, Information and Communication Engineers (IEICE) of Japan. He was a recipient of the 2011 Young Researchers Award by IEICE. He served as a Technical Program Committee (TPC) Member of the IEEE Compound Semiconductor Integrated Circuits Symposium (CSICS) from 2014 to 2017. He has been serving as a TPC Member of the IEEE BiCMOS and Compound Semiconductor Integrated Circuits and Technology Symposium (BCICTS) since 2018 and the IEEE International Solid-State Circuits Conference (ISSCC) since 2019.

Hiroshi Yamazaki (Member, IEEE) received the B.S. degree in integrated human studies and the M.S. degree in human and environmental studies from Kyoto University, Kyoto, Japan, in 2003 and 2005, respectively, and the Dr.Eng. degree in electronics and applied physics from the Tokyo Institute of Technology, Tokyo, Japan, in 2015. In 2005, he joined NTT Photonics Laboratories, Atsugi, Japan, where he has been involved in the research on optical waveguide devices for communication systems. He is concurrently with NTT Network Innovation Laboratories, Yokosuka, Japan, and the NTT Device Technology Laboratories, Atsugi, Japan, where he is involved in the research on devices and systems for optical transmission using advanced multilevel modulation formats. Dr. Yamazaki is a member of the Institute of Electronics, Information and Communication Engineers (IEICE) of Japan.

Hideyuki Nosaka (Member, IEEE) received the B.S. and M.S. degrees in physics from Keio University, Yokohama, Japan, in 1993 and 1995, respectively, and the Dr.Eng. degree in electronics and electrical engineering from the Tokyo Institute of Technology, Tokyo, Japan, in 2003. He joined NTT Wireless System Laboratories, Yokosuka, Japan, in 1995, where he was engaged in the research and development (R&D) of monolithic microwave ICs and frequency synthesizers. Since 1999, he has been involved in the R&D of ultrahigh-speed mixed-signal ICs for optical communications systems with NTT Photonics Laboratories, Atsugi, Japan. He is currently a Senior Research Engineer, a Supervisor, and the Group Leader of the High-Speed Analog Circuit Research Group, NTT Device Technology Laboratories, Atsugi, Japan. Dr. Nosaka is a member of the Institute of Electronics, Information and Communication Engineers (IEICE) of Japan. He was a recipient of the 2001 Young Engineer Award and the 2012 Best Paper Award presented by IEICE. He served as a Technical Program Committee (TPC) Member of the IEEE Compound Semiconductor Integrated Circuits Symposium (CSICS) from 2011 to 2013, and the IEEE International Solid-State Circuits Conference (ISSCC) from 2013 to 2017. He has been serving as a member of the IEEE MTT-S Technical Committee on RF/Mixed-Signal Integrated Circuits and Digital Signal Processing (MTT-15).

Yutaka Miyamoto (Member, IEEE) received the B.E. and M.E. degrees in electrical engineering from Waseda University, Tokyo, Japan, in 1986 and 1988, respectively, and the Dr.Eng. degree in electrical engineering from Tokyo University, Tokyo, Japan, in 2016. He joined NTT Transmission Systems Laboratories, Yokosuka, Japan, in 1988, where he was engaged in the research and development of high-speed optical communications systems including the 10-Gbit/s first terrestrial optical transmission system (FA-10G) using erbium-doped fiber amplifiers (EDFA) inline repeaters. He was with NTT Electronics Technology Corporation, Yokohama, Japan, from 1995 to 1997, where he was engaged in the planning and product development of high-speed optical module at the data rate of 10 Gb/s and beyond. Since 1997, he has been with NTT Network Innovation Laboratories, Yokosuka, Japan, where he has contributed to the research and development of optical transport technologies based on 40/100/400-Gbit/s channel and beyond. He is currently an NTT Fellow and the Director of the Innovative Photonic Network Research Center, NTT Network Innovation Laboratories, where he has been investigating and promoting the future scalable optical transport network with the Pbit/s-class capacity based on innovative transport technologies such as digital signal processing, space division multiplexing, and cutting-edge integrated devices for photonic preprocessing. Dr. Miyamoto is a Fellow of the Institute of Electronics, Information and Communication Engineers (IEICE).